Capturing the sampling effects: *a TOD sensor performance model*

Maarten A. Hogervorst[*a], Piet Bijl[a], J. Mathieu Valeton[a]

[a]TNO Human Factors, Kampweg 5, 3769 DE Soesterberg, The Netherlands

ABSTRACT

The standard way to characterize sensor performance is by means of the Minimum Resolvable Temperature Difference (MRTD) and Minimum Resolvable Contrast (MRC) methods. These methods are based on Fourier analysis and work reasonably well for linear (analogue) systems. However, nonlinear effects, such as sampling, are not properly accounted for. As an alternative, the Triangle Orientation Discrimination (TOD) method has been proposed, based on 4 oriented triangles, that can handle nonlinear effects.

Here, we present a model that predicts the TOD-sensor performance characterization curve from the system parameters. It consists of i) a sensor model and ii) a model of the visual system of the observer. The sensor model generates display images which are fed into the visual system model. The visual system is modeled by a bank of band-pass filters which mimic the pattern of neural activity in the visual cortex (using a common stack model). The neural activity is calculated and internal noise is added. Finally, a decision is made based on a correlation with the expected neural activity of the 4 possible inputs.

The model has been validated with two human observer experiments in which the TOD-curve 1) of the naked eye, and 2) of a simulated thermal staring sensor system were measured. An internal noise level could be found for which the TOD of the naked eye of the two observers could be predicted. The model gives reasonable (but somewhat optimistic) predictions of the TOD-sensor performance curve of the simulated staring camera. Although more tests and modifications are required, these preliminary results suggest that the model can be developed into a model which predicts the TOD for all kinds of sensor systems, which may include sampling effects, noise, blur and (local) image enhancement methods.

Keywords: electro-optical system performance testing, TOD methodology, infrared, visual performance, detection, recognition

1 INTRODUCTION

The traditional end-to-end thermal imager performance measure, the MRTD (Minimum Resolvable Temperature Difference), which has been developed for the first generation or scanning imagers, is unable to adequately predict Target Acquisition (TA) performance for second generation or staring imagers [1,2,3]. The reason is, that the image of a staring sensor is usually under-sampled which causes artifacts that are essentially different for the periodic four-bar pattern that is used in the MRTD procedure than for real targets. Theoretically, the maximum allowed MRTD spatial frequency for staring sensors is half the sample frequency of the Focal Plane Array (FPA). As a consequence, there is no basis to assume a one-to-one relationship between MRTD and acquisition of real targets. Experimental data also show that, when the translation from MRTD to field performance for scanning systems (known as the 'cycle criteria' or 'Johnson criteria'), is applied to staring systems, this generally leads to far too pessimistic range predictions.

Recently, three promising alternative Sensor Performance Measures have been proposed: the TOD[1,2,4] (Triangle Orientation Discrimination threshold), the MTDP[5] (Minimum Temperature Difference Perceived) with the TRM3 model, and the NVtherm model[6]. An overview of the approaches is given by Bijl et al.[7] and the status of TRM3 and NVTherm is outlined by Driggers et al.[8]. For a Sensor Performance Measure it is important that it satisfies three criteria: (i) it should have a solid laboratory measurement procedure, (ii) the lab measure has to be representative for field performance, and (iii) there should be a model that predicts the lab measure from the sensor parameters.

[*] Correspondence: hogervorst@tm.tno.nl, Phone (+) 31 346 356237, Fax (+) 31 346 53977

With respect to the *laboratory measurement*, it appears that the TOD is the best of the three alternatives. It is suitable for all types of imaging systems, is characterized by a solid measurement procedure and an easy observer task, and is representative for a real TA task. Experimental assessment of the TOD is much easier than e.g. measuring an MRTD, and the results are more accurate. The MTDP for example depends on the subjective criterion of the observer, and for the NVTherm approach there is not yet a laboratory measurement available.

Further, the TOD seems to correspond to *field performance* very well. In a first validation study[9] it was shown that the shape of the TOD for a CCD camera matches the relationship between contrast and TA range for ship targets. A second study[8] showed that the TOD predicts TA performance differences between scanning and staring thermal imagers of different types very well.

What is still missing is a TOD sensor performance model, i.e. a model that predicts the TOD-sensor performance curve from the physical parameters of the sensor system. In the current paper we will present such a model. We also present some preliminary experiments to validate the model.

2 GENERAL MODEL DESCRIPTION

The model consists of a) a sensor model and b) a vision model. The sensor model generates display images from the physical parameters of the sensor system. These display images are fed into the vision model in which human processing of the display image is modeled. It is a spatial model, meaning that for a certain point in time a display image is generated (containing noise). In the vision model this (noisy) display image is processed further, which involves addition of internal noise. Predicted human performance is calculated through Monte Carlo simulation, i.e. for each stimulus level many display images are generated and many mental images (the pattern of neural activity which includes internal noise) are calculated and processed. The output of the model is the probability of a correct answer. From this the 75% percent threshold can be deduced.

The model is implemented in MatLab. Discretely sampled images are used as input. The sample size is determined by the sample size of the vision model. We used a sample size of 0.153 mrad (visual angle), which resembles the spacing of the cones in the fovea[10, 11].

3 SENSOR MODEL

To model the sensor system parts of the Night Vision Thermal Imaging System Performance Model (NVTherm)[12, 13, 14] are used. The input of this model consists of the physical parameters of the sensor, such as parameters of the lens (f-number, transmission, optics blur spot etc), system (e.g. viewing angle), electronics, detector (e.g. size) and display (e.g. display spot size). The output contains the 1-D (horizontal & vertical) Modulation Transfer Functions (MTFs) which are used to model the linear stages of the sensor model. In most cases the 2-D MTFs are derived from these 1-D MTFs by simple (matrix) multiplication. The 2-D optics MTF is calculated by using the equations used by NVTherm, since the product of the 1-D MTFs is not circularly symmetric and therefore unrealistic. In our model the sampling stage is made explicit. The following stages are modeled:

- optics (a form of pre-sample blur).
- sampling: which consists of i) convolution by the detector response function and ii) discrete sampling.
- addition of detector noise
- sample & hold: the transformation into an analogue signal
- electronics and display (the post-sample blur).

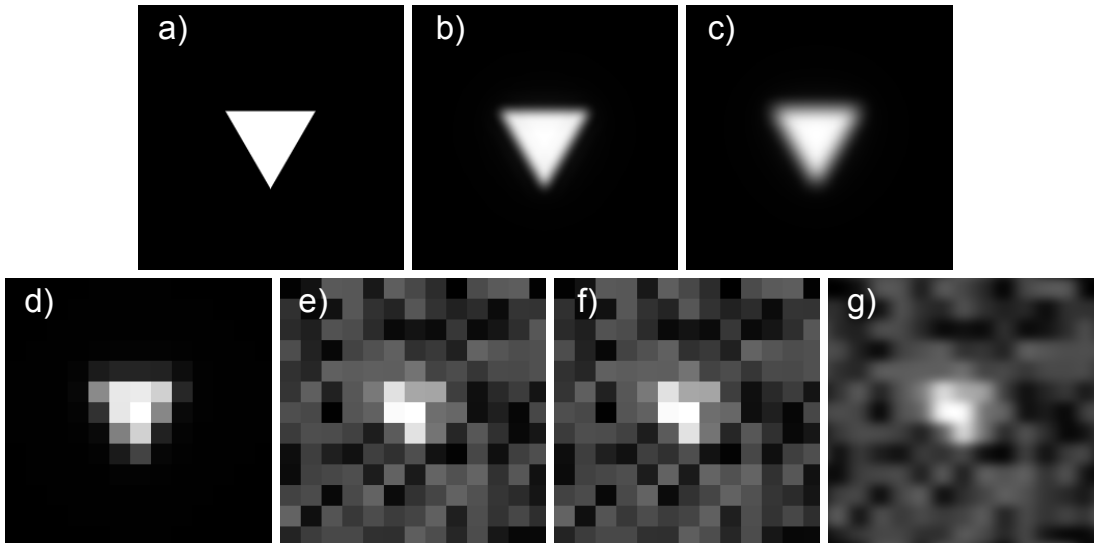

Figure 1. The image in various stages of the sensor model. From input image (a) to display image (g): a) input image, b) distorted by optics, c) after convolution with detector response function, d) sampled values, e) after addition of detector noise, f) sample & hold, g) distorted by electronics and display blur.

3.1 Optics

The effect of the optics is modeled by multiplication of the Fourier transform of the image by the optics-MTF (see Figure 1b). As mentioned above, the 2-D optics MTF is calculated directly from the equations used by NVTherm. The diffraction limited optics MTF is given by:

$$H_{odl}(f_s) = \frac{2}{\pi}\left(\arccos\left(\frac{\lambda f_s}{D_o}\right) - \left(\frac{\lambda f_s}{D_o}\right) * \sqrt{1-\left(\frac{\lambda f_s}{D_o}\right)^2} \right), \qquad (1)$$

in which f_s is the spatial frequency in [cycles/mrad], λ is the wavelength for diffraction [μm] and D_o is the optics aperture [mm]. The geometric blur MTF is given by (assuming Gaussian blur):

$$H_{ogb}(f_s) = e^{-2\pi^2\sigma^2 f_s^2} \quad , \qquad (2)$$

in which σ equals the width of the Gaussian distribution [mrad]. The total optics MTF is the product of these two MTFs.

3.2 Sampling

The optical signal is transformed into a discrete number of samples by the detectors. The effect of sampling is modeled by convolution with the detector response function (which in this case is a simple block function, i.e. a function which is 1 at the detector and 0 elsewhere), see Figure 1c, followed by sampling at the sample grid locations (Figure 1d). Some variation in relative position between the figure and the grid can be obtained by varying the offset (starting point) of the grid. (The TOD-method requires that the test pattern is offset by a different, random vector from trial to trial.)

3.3 Detector noise

The effect of detector noise is modeled by adding to each of the sampled values a random number between zero and some fixed value (the same for each pixel), drawn from a flat probability distribution[1] (see Figure 1e).

3.4 Sample and hold

The discrete set of values is transformed into an analogue signal through the sample and hold technique. We assume that after this transformation the value is the same over the detector area.

3.5 Electronics and display

The analogue signal is transformed by the electronics and displayed onto the monitor. The effect of this is modeled by multiplication the Fourier transform of the image by the electronics and display MTF's.

3.6 Practice

To speed up the operation the pre- and post sampling MTFs are calculated first. The pre-sampling MTF consists of the product of the optics MTF and the detector-response MTF. The post-sampling MTF consists of the product of the electronics and the display MTFs.

4 VISION MODEL

The display image is fed into the vision model. This model calculates a representation of the image which resembles the neural activity in the human visual cortex. This type of model has become quite common in biological vision, computer vision and image processing[15,16]. We use the Laplacian Pyramid model developed by Burt & Adelson[15]. Each neuron in this model is characterized by a response function which has the shape of a "Mexican hat" (see Figure 2).

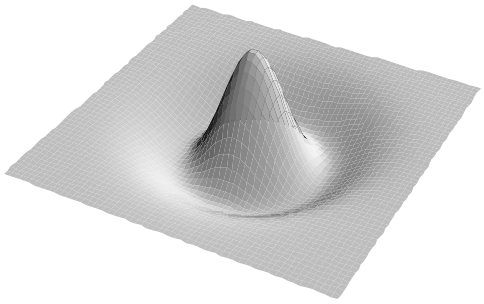

Figure 2. A 3-D graph showing the shape of the response function of a neuron in the vision model. The x and y coordinates specify the retinal position; the z-variable indicates the weight associated with this position. The shape resembles that of a "Mexican hat".

Their output is a weighted sum of the input luminance, in which the weight varies with the position on the retina according to a difference of two Gaussians (DOG). These cells do for instance not respond to uniform light field, since the positive response in the center is cancelled by the negative response to the surrounding. The retinal area over which they sum their inputs is referred to as the receptive field. These neurons act as localized frequency band-pass filters. Their bandwidth is one octave (which makes efficient coding possible). The idea is that i) neurons exist with receptive field sizes which range from small to large and ii) that their density is inversely related to their receptive field size, i.e. in a given retinal area there are fewer neurons with a larger receptive field size.

[1] It might be more correct to draw the noise from a Gaussian probability distribution (or one which applies to the detector). However, the effect of this change in the model is likely to be small, since many samples are drawn.

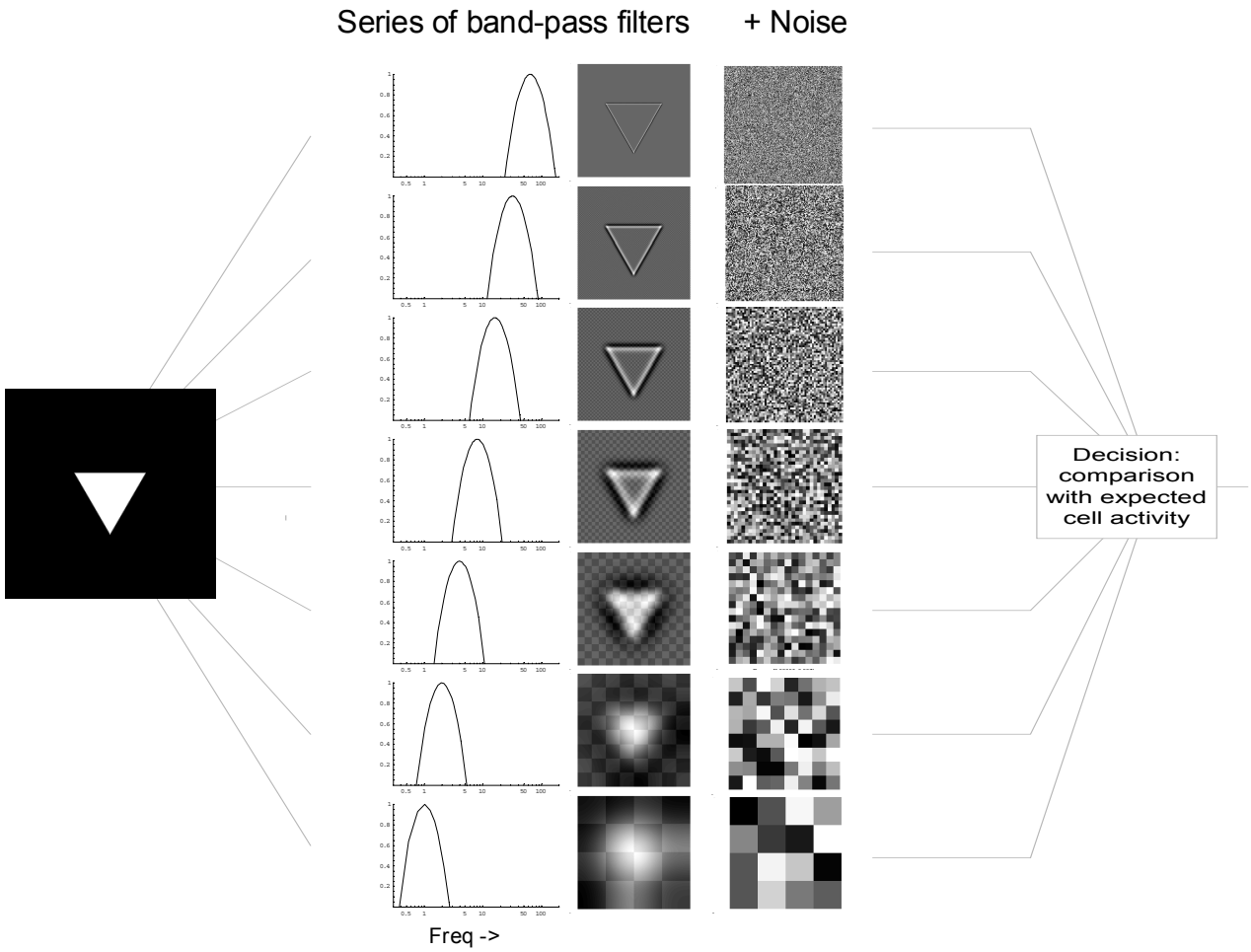

Figure 3. A schematic overview of the vision model. For each input image the activity of a set of neurons is calculated. The first column of images shows the band-pass filtered versions of the input image. The activity of the neurons is represented by the gray level. For a given retinal area the number of neurons decreases with a decrease in center frequency. This is indicated by the increasing size of the checks in the checker board pattern superimposed on the images (i.e. each square represents a neuron). The second column of images represents the next stage in the model, in which the activity of each neuron is perturbed by internal noise. Finally, one of the 4 triangle orientations is chosen based on a comparison of the pattern of neural activity with the expected pattern of activity (see text for details).

Figure 3 gives a schematic overview on the various stages involved in the vision model. The different parts are discussed below in detail.

4.1 Input

The input to the model consists of the contrast image, i.e. the luminance L divided by the average background luminance L_{back}, i.e. L/L_{back}. The retinal image is first transformed into a sampled image, in which the pixel size (width and height) is equal to 0.153 mrad. This resembles the cone spacing in the fovea and determines the highest frequency that can be detected by the system. It is derived from the model by Geisler & Davila[10,11], in which a densely packed triangular array of cones was assumed. (The Nyquist frequency of this model is 57 cycles/deg.)

4.2 Laplacian Pyramid decomposition

Firstly, the image is decomposed into a Laplacian Pyramid: a series of frequency band-passed images in which the width and height decrease by a factor 2 when going to a lower scale. This means that the number of neurons (in a given retinal area) decreases with decreasing center frequency. This is represented in Figure 3 by the decrease in the number of squares of the checker board pattern superimposed on the images.

4.3 Internal noise

The activity of each neuron is perturbed by internal noise. A random number drawn from a flat probability distribution of fixed magnitude and zero average is added to each activity level. The noise on each neuron is the same.

4.4 Decision stage

The (model) observer is forced to choose which of 4 oriented triangles was presented (a triangle with apex UP, DOWN, LEFT or RIGHT: $\nabla \Delta \triangleleft \triangleright$). This choice is based on a comparison between the measured neural activity and the expected neural activity for a given triangle. For 4 template triangles the expected neural activity pattern is calculated. The expected neural activity follows from a Laplacian Pyramid decomposition of images of 4 differently oriented white triangles on a black background (the templates), i.e. for which the stimulus level is 1 at the triangle and 0 (zero) in the background[2]. The resemblance between the measured pattern and the expected pattern is quantified by the correlation (a simple inner product between the two vectors). The model chooses the triangle with the highest correlation value.

5 PSYCHOMETRIC FUNCTION

The probability of correct identification is determined by Monte Carlo simulation. This means that for a given stimulus level, for some instant in time, a probable display image is calculated. For this display image a probable pattern of neural activity is calculated and a decision is made. When this is repeated many times the fraction of correct responses can be determined. When the fraction correct is plotted as a function of the stimulus level a psychometric function is obtained (see Figure 4).

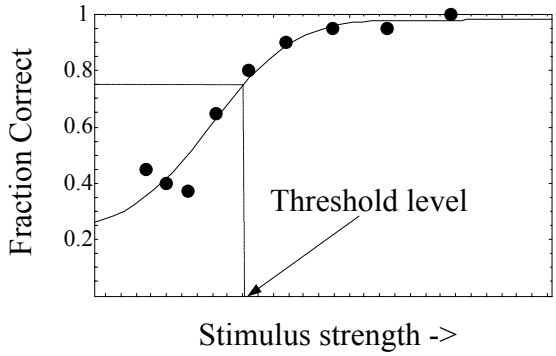

Figure 4. The fraction correct as a function of the stimulus strength (e.g. SNR-level, size or contrast). The fraction of correct responses varies from 0.25 (chance) to nearly 1.00. The dots represent calculated fraction correct. The data is fitted by a Weibull curve and the 75% correct level (the threshold) is determined.

To obtain the fraction correct at a given stimulus strength the following procedure is followed:

- First an image is generated of a triangle with certain orientation in which the center is displaced horizontally and vertically by a random amount between –0.5 and +0.5 pixels. We used anti-aliased triangles, i.e. defined at sub-pixel resolution.
- The image is presented at a random position with respect to the detector grid and a probable display image is calculated.
- The display image is fed into the vision model: a probable pattern of neural activity is calculated, compared to the expected activities, and the most probable of the 4 orientations is chosen.

For each stimulus strength this procedure is repeated many times. The templates remain fixed, such that the expected activities only have to be calculated once. The scores are calculated for various stimulus strengths[4] to create a psychometric curve. A Weibull function is fitted through the data:

$$p(x) = (1-\delta) - (1-\delta-\gamma) * 2^{-(x/\alpha)^{\beta}}, \qquad (3)$$

[2] The figures are displaced by +/- 0.5 pixel relative to the (cones) grid of the visual system. To account for some uncertainty in the position of the test pattern, templates are used which are blurred by a Gaussian with a sigma of 1.2 pixel.

in which $p(x)$ is the probability of correct identification for stimulus level x, δ is the error rate at high stimulus levels, γ is score at chance level, and α and β indicate the threshold and the slope.
From this fit the 75% threshold level and the error in this are deduced.

6 VALIDATION EXPERIMENTS

In order to validate the model two experiments were conducted in which human observer performance was compared to the model predictions:

1) TOD-curve for the naked eye. In this experiment the sensitivity for triangles of different contrasts and sizes was determined for two observers without sensor system. This experiment gives a good insight in the internal noise level of the visual system, since no external noise is added.
2) TOD-curve for a simulated staring camera. For various sizes the performance was measured as a function of signal to noise ratio (SNR). Also, the threshold size (acuity) was determined. In this experiment, human performance is governed by the external noise of the sensor system.

7 TOD FOR NAKED EYE

7.1 Method

The observer was positioned at a large distance (800cm) from a computer screen (i.e. the smallest test patterns were well defined) with two eyes open. On the monitor triangles of various sizes were displayed. (The size is defined as the square root of the area.) The luminance output of the screen was linearized and defined at 12 bits resolution, and the test patterns were displayed against a uniform background luminance of 22 cd/m^2. (The monitor was seen through an aperture in a slide projector screen to create a large field in which the luminance was the same as the background.) The figures gradually appeared (in 133 msec), stayed on for a short time (533 msec), and gradually disappeared (in 133 msec). For a given contrast test patterns of positive and negative contrast were displayed at random. After each trial the observer indicated the orientation of the triangle by pressing one of 4 buttons. Each trial took approximately 1.5 seconds and it took about 4 min. to obtain a psychometric curve (30 samples at 7 stimulus levels). The data of 3 such curves were averaged. At a fixed contrast of 100% the acuity (smallest recognizable triangle) was measured, and at 6 triangle sizes the threshold contrast was determined. See Bijl & Valeton[4] for a detailed description of the measurement procedure.

7.2 Results

Figure 5 shows the TOD-sensitivity curves for the 2 observers along with the predictions of the model for 2 internal noise levels (0.5 and 0.25). The TOD-curve of observer PB is lower than the TOD-curve of observer MAH. The data of observer MAH is reasonably well predicted by the model with an internal noise level of 0.5. When the internal noise level is reduced by a factor of 2 the model prediction resembles the data of observer PB. The differences between the two observers' sensitivity can be explained from a difference in internal noise level.

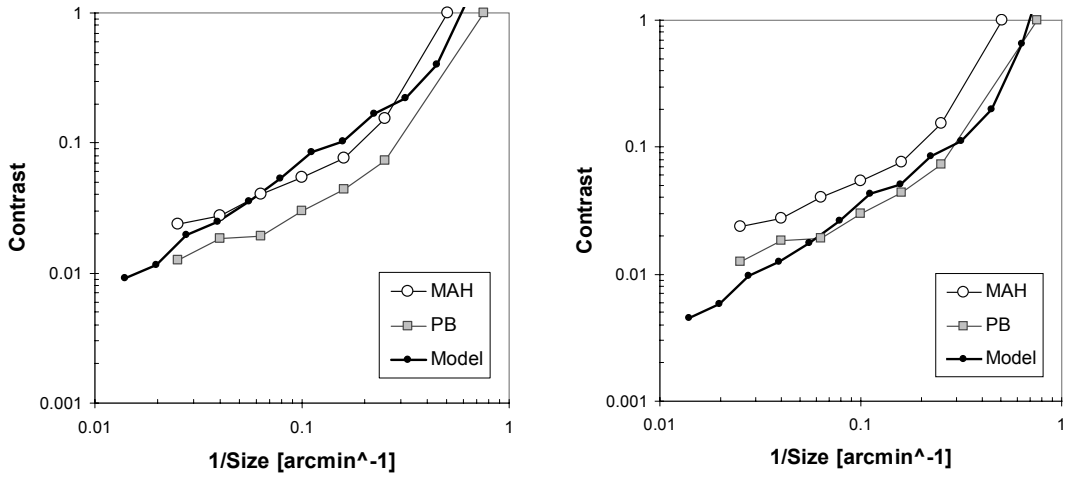

Figure 5. The TOD-sensitivity curves for 2 observers (MAH and PB) along with the predictions of the model for noise levels of 0.50 (left) and 0.25 (right).

8 TOD FOR A SIMULATED STARING CAMERA

8.1 Method

A staring camera was modeled with parameters specified in the file "star" supplied with the NVTherm program as an example of a thermal staring sensor (e.g. wavelength range 3-5 μm, detector field of view size of 0.234 arcmin). Our sensor model (which uses the NVTherm.exe program) was used to calculate a number of (noisy) sample display images. These images were displayed on a standard computer monitor at high contrast and a distance of 35 cm (one for each trial). Each detector of the sensor filled 6x6 pixels of the PC monitor, showing clearly the effect of blur from the post-sampling MTF. The acuity threshold (smallest triangle) was determined as well as the Signal-to-Noise ratio for 4 triangle sizes.

8.2 Results

Figure 6 shows the thresholds obtained from observer MAH and PB along with the model predictions of a model with internal noise levels of 0.5 (Model_MAH) and 0.25 (Model_PB). (The noise level used in the SNR ratio is equal to the standard deviation of the (flat) distribution.) The model predictions of the two models are quite similar. The thresholds obtained from observer PB are also very similar, but somewhat higher (48%), than those from observer MAH. This suggests that performance in this experiment is governed by external noise rather than internal noise in the observer. This feature is predicted well by the model.

The measured acuity threshold is predicted quite well. The predicted SNRs are somewhat lower than the measured ones (on average by 48% for MAH, and by 77% for PB), i.e. the model performs too well.

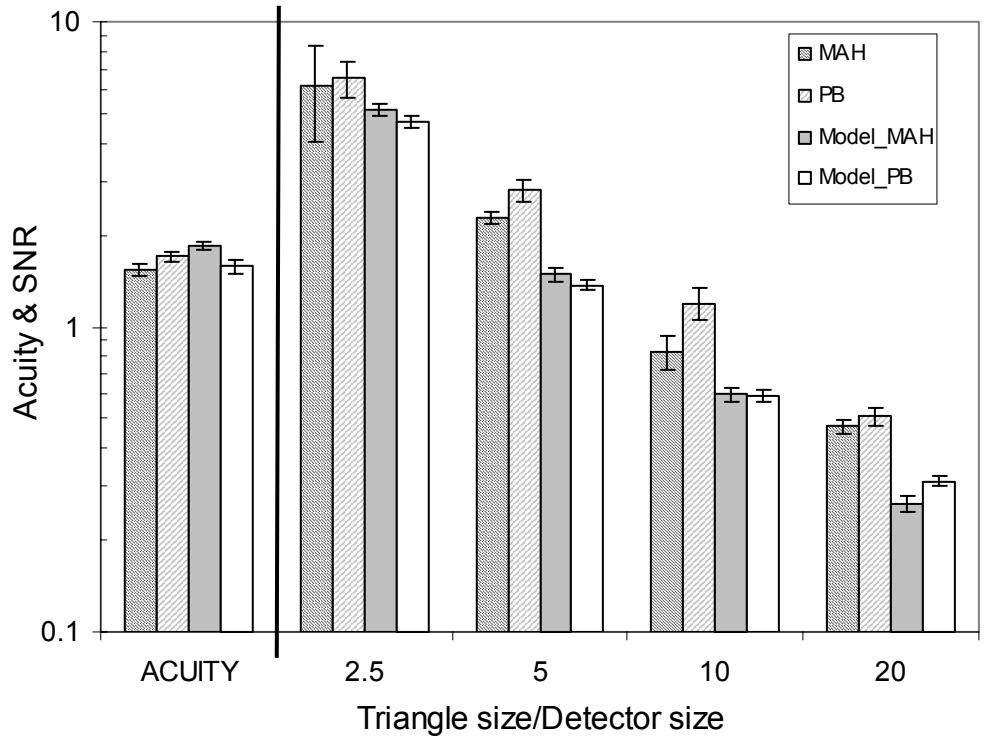

Figure 6. Measured thresholds for a simulated staring camera along with the predictions of the model. Shown are the acuity (smallest recognizable size) and the threshold signal-to-noise (SNR) levels for 4 triangles sizes. The sizes and acuity are expressed in units of the detector size of the sensor system.

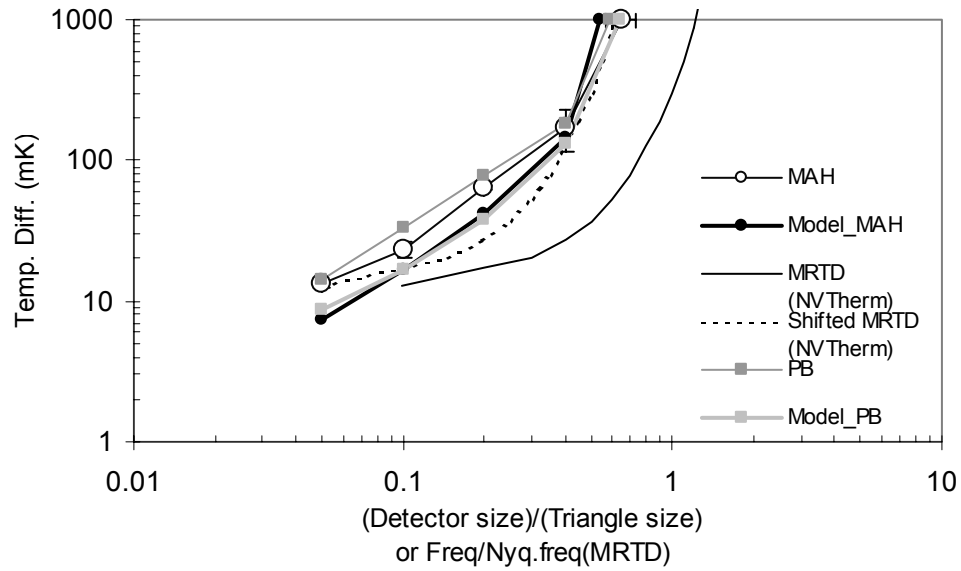

Figure 7. The threshold data from Figure 6 transformed into a TOD-curve with noise estimates from NVTherm. The acuity data (obtained without noise) are (arbitrarily) placed at a temperature difference of 1000 mK. Threshold temperature differences are plotted as a function of the inverse of the triangle size in detector size units (the 2 observers and models). Also plotted is the MRTD as predicted by NVTherm as a function of the spatial frequency (divided by the Nyquist frequency of the sensor). In the shifted version the frequency is multiplied by 0.5 (see text).

Figure 7 plots the same SNR-thresholds, but now transformed into threshold temperature differences using noise estimates from NVTherm. The acuity data (obtained without noise) are (arbitrarily) placed at a temperature difference of 1000 mK. Threshold temperature differences are plotted as a function of the inverse of the triangle size in detector size units (observer MAH and the model).

The SNR levels were converted into threshold temperature differences $\Delta T_{thresh.}$ by:

$$\Delta T_{thresh.} = SNR * NETD * k \,, \qquad (4)$$

in which *NETD* is the Noise Equivalent Temperature Difference, in this case 16 mK, and *k* is a multiplication factor which is 1.75 here. The magnitude of factor *k* is based on the assumption that the noise is largely a combination of dynamic noise (σ_{tvh}) and static (fixed pattern) noise (σ_{vh}), and that the latter is 0.4 times as large as the dynamic noise (standard estimates used by NVTherm for this type of sensor). We further assume an integration time of 100 msec (6 frames). An estimate of the total noise in the average is therefore $\sigma_{tot} = \sqrt{\left(\frac{\sigma_{tvh}}{\sqrt{6}}\right)^2 + \left(0.4\,\sigma_{tvh}\right)^2} \approx \frac{1}{1.75}\,\sigma_{tvh}$, i.e. $\sigma_{tvh} = 1.75\,\sigma_{tot}$.

Also plotted is the predicted Minimum Resolvable Temperature Difference (MRTD) of a 4 bar pattern as predicted by NVTherm as a function of normalized spatial frequency (i.e. divided by the Nyquist frequency of the sensor). The shape of the TOD-curve is similar to that of the MRTD (although the MRTD-curve appears to level off faster than observed, similar to what was observed previously by Bijl & Valeton[9]). Because the test patterns are different their sensitivity curves do not have to match directly. By multiplying the frequency by a factor of 0.5 the curves approximately match.

9 DISCUSSION

We have presented a TOD-sensor performance model which consists of a sensor model and a vision model. The sensor model is partly based on the (thoroughly-validated) NVTherm model. We have also presented a plausible model of human visual processing based on a commonly used model of the neural activity in the visual cortex. Instead of comparing the retinal image with templates directly, a representation of the neural activity is compared with the expected pattern of each template. We have performed two preliminary experiments in order to validate the model. For suitably chosen internal noise levels the TOD-sensitivity curve for the naked eye of two observers could be predicted. The model also gives reasonable (albeit too optimistic) predictions for the TOD-curve of a simulated staring sensor.

The model we propose is a spatial model and performance is determined through Monte Carlo simulation. The advantage of such a model is that nonlinear effects can be dealt with in a simple and straightforward manner. This means that sampling effects and other nonlinearities in the system can be accounted for. Moreover, it can be expected that image enhancement techniques will become increasingly important, in which often highly nonlinear image transformations are used. Such effects can be incorporated into the model (although different tests have to be devised to test the effect of local image transformations). The model is relatively computationally expensive (compared to the NVTherm model). However, the computational power of current (and especially future) PCs is high enough to get quick results.

The model is separated into two parts: a sensor model and a vision model. This has the advantage that each of these parts can be used on its own. Various human observer experiments can be performed using the simulated sensor to obtain human performance measures for a wide range of tasks and circumstances. The vision model can be applied directly to frames grabbed from a display. This makes the separate estimation of various sensor parameters superfluous. Also, when a better model for each of these parts comes available this part can be easily replaced.

Not only does the model predict the 75% correct threshold, it predicts the percentage correct at different stimulus levels. This means that a different threshold level can be chosen. In practice it may be required to choose a much higher confidence level. It can be expected that there is not always a direct relation between the 75% (or 50%, as calculated in NVTherm) correct threshold and the stimulus level required for a much higher performance level.

The model is still under development and more testing and alterations will be necessary before the model will be able to successfully predict sensor performance in a wide range of situations. It might for instance be better to use a model in which oriented filters are used, or the system might use only the neurons which are informative. Still, the current results (and the success of this type of model in explaining other human vision experiments) suggest that this model has good potential in growing into a valuable tool for assessing sensor performance. It makes the TOD method a good alternative to the standard MRTD method.

10 ACKNOWLEDGEMENT

We wish to thank our colleagues at the U. S. Army Night Vision & Electronics Directorate for supplying us documentation and software about NVTherm.

11 REFERENCES

1. P. Bijl and J.M. Valeton, "TOD, a new method to characterize electro-optical system performance". *Proc. SPIE*, **3377**, 182-193, 1998.
2. P. Bijl and J.M. Valeton, "TOD, the alternative to MRTD and MRC". *Optical Engineering*, **37**(7), 1984-1994, 1998.
3. Driggers, R.G., Vollmerhausen, R. & Halford, C.E. "Sampled Imaging Systems". *Optical Engineering* **38** (5), 740 – 741, 1999.
4. Bijl, P.& Valeton, J.M. "Guidelines for accurate TOD measurement", *Proc. SPIE*, **3701**, 14-25, 1999
5. Wittenstein, W., " Minimum temperature difference perceived – a new approach to assess undersampled thermal imagers". *Optical Engineering*, **38** (5), 773 – 781, 1999.
6. Vollmerhausen, R., Driggers, R.G. & O'Kane, B.L. "Influence of sampling on target recognition and identification". *Optical Engineering*, **38** (5), 763 – 771, 1999.
7. Bijl, P., Valeton, J.M. & Hogervorst, M.A. "A critical evaluation of test patterns for EO system characterization". *Proc. SPIE*, **4372**, 2001 (this issue).
8. Driggers, R.G., Vollmerhausen, R., Wittenstein, W., Bijl, P., Valeton, J.M. "Infrared Imager Models for Undersampled Imaging Systems". *Proc. Fourth Joint International Military Sensing Symposium*, **45** (1), 335-246, 2000.
9. Bijl, P.& Valeton, J.M. "Validation of the new TOD method and ACQUIRE model predictions using observer performance data for ship targets". *Optical Engineering*, **37** (7), 1984 – 1994, 1998.
10. Geisler, W.S., Davila, K.D., "Ideal discriminators in spatial vision: two-point stimuli", *Opt. Soc. Am. A*, **2**, 1483, 1985.
11. De Lange, D.J., Valeton, J.M., Bijl, P. "Automatic characterization of electro-optical sensors with image processing, using the Triangle Orientation Discrimination (TOD) method", *Proc. SPIE,* **4030**, 104-111, 2000.
12. Vollmerhausen, R., NVTherm.exe, version 23 sept. 1999.
13. Vollmerhausen, R., "Incorporating display limitations into night vision performance models", *IRIS Passive Sensors*, March, 1995.
14. Vollmerhausen, R., Driggers, R., "Modeling the Target Acquisition Performance of Staring Array Imagers", *IRIS Passive Sensors*, March, 1998.
15. Burt, P.J., Adelson, E.H., "The Laplacian pyramid as a compact image code", *IEEE Trans. Commun*, **31** (4), 532-540, 1983.
16. Watson, A.B., "The Cortex Transform: Rapid Computation of Simulated Neural Images", *Computer Vision & Image Processing*, **39**, 311-327, 1987.